EXPERIMENTAL CELL RESEARCH 315 (2009) 1850–1859

available at www.sciencedirect.com

ScienceDirect

www.elsevier.com/locate/yexcr

Research Article

Endothelial monocyte activating polypeptide-II modulates endothelial cell responses by degrading hypoxia-inducible factor-1alpha through interaction with PSMA7, a component of the proteasome

Anita T. Tandle[a], *Maura Calvani*[b], *Badarch Uranchimeg*[b], *David Zahavi*[a], *Giovanni Melillo*[b], *Steven K. Libutti*[c,*]

[a]*Tumor Angiogenesis Section, Surgery Branch, Center for Cancer Research, National Cancer Institute, Bethesda, Maryland 20892, USA*
[b]*DTP-Tumor Hypoxia Laboratory, SAIC Frederick, Inc., National Cancer Institute, Frederick, Maryland 21702, USA*
[c]*Department of Surgery, Montefiore-Einstein Center for Cancer Care, Albert Einstein College of Medicine, Greene Medical Arts Pavilion, 4th Floor 3400, Bainbridge Avenue, Bronx, New York 10467, USA*

ARTICLE INFORMATION

Article Chronology:
Received 17 November 2008
Revised version received
16 March 2009
Accepted 30 March 2009
Available online 10 April 2009

Keywords:
Angiogenesis
EMAP-II
HIF-1α
Proteasome
Integrin receptor

ABSTRACT

The majority of human tumors are angiogenesis dependent. Understanding the specific mechanisms that contribute to angiogenesis may offer the best approach to develop therapies to inhibit angiogenesis in cancer. Endothelial monocyte activating polypeptide-II (EMAP-II) is an anti-angiogenic cytokine with potent effects on endothelial cells (ECs). It inhibits EC proliferation and cord formation, and it suppresses primary and metastatic tumor growth in-vivo. However, very little is known about the molecular mechanisms behind the anti-angiogenic activity of EMAP-II. In the present study, we explored the molecular mechanism behind the anti-angiogenic activity exerted by this protein on ECs. Our results demonstrate that EMAP-II binds to the cell surface α5β1 integrin receptor. The cell surface binding of EMAP-II results in its internalization into the cytoplasmic compartment where it interacts with its cytoplasmic partner PSMA7, a component of the proteasome degradation pathway. This interaction increases hypoxia-inducible factor 1-alpha (HIF-1α) degradation under hypoxic conditions. The degradation results in the inhibition of HIF-1α mediated transcriptional activity as well as HIF-1α mediated angiogenic sprouting of ECs. HIF-1α plays a critical role in angiogenesis by activating a variety of angiogenic growth factors. Our results suggest that one of the major anti-angiogenic functions of EMAP-II is exerted through its inhibition of the HIF-1α activities.

Published by Elsevier Inc.

Introduction

Angiogenesis, the growth of new blood vessels, is essential for pathological processes such as tumor growth and metastasis, proliferative retinopathies, age-related macular degeneration, and rheumatoid arthritis [1]. Endothelial cells (ECs) play a key role in all aspects of angiogenesis [2]. Understanding specific mechanisms that contribute to angiogenesis offer the best approach to develop therapies to inhibit angiogenesis in cancer and other related diseases.

* *Corresponding author.*
E-mail address: slibutti@montefiore.org (S.K. Libutti).

0014-4827/$ – see front matter. Published by Elsevier Inc.
doi:10.1016/j.yexcr.2009.03.021

Hypoxia is an important regulator of blood vessel tone, vessel structure and has been shown to be a potent stimulus of angiogenesis. It regulates genes that are involved in angiogenesis, vasculogenesis, glucose metabolism and apoptosis [3]. An important master regulator of angiogenesis under hypoxic conditions is hypoxia-inducible factor-1 (HIF-1), a dimeric transcription factor composed of HIF-1α and HIF-1β [4]. HIF-1α controls critical pro-angiogenic growth factors such as vascular endothelial growth factor (VEGF), VEGF-receptor, and erythropoietin [3–5]. Hypoxic stabilization of HIF-1α resulting in chemo- and radio-resistance is a hallmark of the majority of solid tumors [6]. The identification of the molecular mechanism of HIF-1α regulation has several implications regarding the potential treatment of several diseases.

Endothelial monocyte activating polypeptide-II (EMAP-II) is a pro-inflammatory cytokine with potent effects on ECs. It induces tissue factor (TF) expression to modulate coagulant responses, induces the expression of P- and E-selectin and upregulates tumor necrosis factor-α (TNF-α) receptors [7–9]. It inhibits EC proliferation, migration, angiogenic cord formation and induces apoptosis [10]. EMAP-II treatment induces a TNF-like thrombohemorrhage and renders TNF-α resistant tumors sensitive to systemic TNF-α therapy [7,11,12]. Upregulation of EMAP-II directly after isolated limb perfusion (ILP) of melanoma patients predicts a complete response to TNF-α, suggesting that the EMAP-II is critical for the antitumor activity of TNF-α [13]. The effects are thought to be the result of EMAP-II's activity on ECs.

The various effects of EMAP-II on ECs suggest an important role for EMAP-II in regulating tumor vasculature. However, there are few published papers describing the mechanism of EMAP-II activity on ECs. The present study sheds light on one of the important mechanisms behind the anti-angiogenic activity of EMAP-II.

Materials and methods

Cell culture

Human umbilical vein endothelial cells (HUVEC) were obtained from Cambrex (New Jersey) and cultured in Endothelial Cell Growth Medium-2 as described earlier [14]. All experiments were conducted with HUVEC in passage 3. Human 293 cells were grown in Dulbecco's modified eagle medium with 10% serum, 2 mM glutamine, 100 U/ml penicillin, 100 μg/ml streptomycin, 100 μg/ml gentamicin and fungizome.

DNA constructs

The HIF-1α expression plasmid, pFLAG$_3$HIF-1α was a kind gift from Dr. Gregg Semenza (the Johns Hopkins Institute for Cell Engineering) [15]. A plasmid encoding mature EMAP-II (pAAVEMAP-II) was constructed by amplifying mature EMAP-II from plasmid pET-20b-EMAP-II using primers with NotI and HindIII sites at 5′ and 3′, respectively. The resulting PCR product was subcloned into an adeno associated virus 5 backbone. The pAAV-GFP plasmid constructed in a similar way was used as a control DNA.

Purification of EMAP-II protein

DH5α cells transformed with the pET-20b plasmid, expressing mature EMAP-II as a histidine tagged protein were obtained from Paul Schimmel (the Scripps Research Institute, La Jolla, CA). EMAP-II protein was purified as described earlier [14].

Biotinylation of proteins

Biotin labeling was performed by incubating EMAP-II or bovine serum albumin (BSA) with 10 mM solution of EZ-Link Sulfo-NHS-Biotin (Pierce, Illinois) for 2 h on ice. The unlabeled biotin was removed by passing the mixture through Microcon YM-10 filter units (Millipore, Billerica, Massachusetts).

Flow cytometry

1×10^5 HUVEC were incubated with 0.5 μg of biotinylated EMAP-II for various time points and the binding was detected using Avidin-FITC by flow cytometry. Avidin-FITC reagent, biotinylated bovine serum albumin (BSA) and an isotype control antibody were used as controls. In the competition inhibition experiment, in addition to biotinylated EMAP-II, cells were incubated with either non-biotinylated EMAP-II or anti-α5β1 antibody (Clone JBS5, Millipore, Billerica, Massachusetts) at various concentrations; 0.1 μg, 1 μg and 10 μg.

Immunofluorescence analysis

The EMAP-II binding to EC surface was examined as described by Chang et al. [16]. Briefly, 1×10^6 cells were incubated with 5.0 μg of either biotinylated EMAP-II or BSA for 1 h. In the competition inhibition experiment, in addition to biotinylated EMAP-II, cells were incubated with non-biotinylated EMAP-II at various concentrations; 10 μg and 75 μg. The binding was visualized using Avidin-FITC (Pierce, Illinois). The nuclei were stained using 300 mM DAPI for 2 min, followed by visualization under Zeiss Axiovert S100 fluorescent microscope (Carl Zeiss Inc. Germany).

Cell fractionation

$3–5 \times 10^6$ HUVEC were treated with EMAP-II (0.5 μg for 1×10^5 cells) for different time points. After incubation, cells were fractionated to collect different cellular fractions using ProteoExtract subcellular proteome extraction kit (Calbiochem, California) using the manufacturer's protocol. The fractions were concentrated by passing through Microcon YM-10 filter units and quantitated. 30 μg of each fraction was loaded and subjected to western analysis. In the internalization inhibition experiment, cells were preincubated with either an isotype control antibody, anti-α5β1 (Clone JBS5) or control β1 antibody (Clone LM534) (Millipore, Billerica, Massachusetts) before incubating with EMAP-II.

Western analysis

Total cell lysates were prepared from 293 or HUVEC cells using the lysis buffer (50 mM Tris pH 7.4, 140 mM NaCl, 0.1% SDS, 1% NP40 and 0.5% sodium deoxycholate) containing protease inhibitor cocktail (Roche, Indianapolis). The amount of protein was quantitated using Protein assay reagent from BioRad (BioRad, California). 20 to 30 μg of either a cellular fraction or total lysate electrophoresed on 4–12% Bis-Tris gel (Invitrogen, Carlsbad, California) was transferred to a nitrocellulose membrane and blocked with 5% non-fat milk powder in PBS containing 0.1%

Tween-20. The membranes were incubated with specific primary antibody, followed by a secondary antibody and developed using ECL plus (Amersham, UK). The primary antibodies used were EMAP-II (PeproTech, New Jersey), HIF-1α (BD Biosciences), PSMA7 (BioMol, Pennsylvania), GAPDH, α5β1, α5, and β1 (Millipore, Billerica, Massachusetts) and pan-Cadherin and Histone B (abcam, Cambridge, Massachusetts). The secondary antibodies used were antimouse-horseradish peroxidase (HRP) (Amersham), anti-mouse-alkaline phosphatase (Rockland, Gilbertsville) or anti-goat-HRP (Jackson Laboratories, Maine). Primary antibodies were used at 1:1000 dilutions and secondary antibodies at 1:10,000 dilutions.

Pull down analysis

50 μg of the total cell lysate was incubated with different amounts of purified EMAP-II for 1.5 h at 4 °C. The EMAP-II has a histidine tag at the C-terminus. Thus, bound complexes were pulled down by incubating reactions with 25 μl Ni NTA Superflow beads (Qiagen, Valencia, CA) for 1.5 h at 4 °C. The bound proteins were eluted in NuPAGE LDS sample buffer (Invitrogen, Carlsbad, CA) and immunoblotted.

Peptide competition assay

The following peptides were synthesized (Sigma Genosys, the Woodlands, Texas). Test peptides (spots 41, 42 and 45): spot 41: PLACSPLAAG, spot 42: CSPLAAGQSR, and spot 45: RLRHGGSCHV. Control peptides (spots 3 and 50): spot 3: ITVFSPDGHL and spot 50: AEQWAQAVWH. For the peptide competition assay, a mixture of EMAP-II and HUVEC total cell lysate was incubated with either a cocktail of test peptides or control peptides, followed by a pull down analysis as described.

Transfection assays

293 cells were transfected using lipofectamine 2000 (Invitrogen, Carlsbad, California) with pFLAG$_3$HIF-1α (50 ng) and various combinations of pAAVEMAP-II DNA or control DNA (10 ng, 50 ng and 100 ng) for 24 h. In dual luciferase reporter assay, cells were additionally transfected with 20 ng of pGL2-TK-HRE [17] and 5 ng of *Renilla* plasmid (Promega, Inc., Madison, WI). In proteasome inhibition experiments, cells were incubated with 20 μM of proteasome inhibitor, MG132 (Calbiochem, Gibbstown, NJ) after 4 h of transfection. After a 24 h transfection, cell lysates were prepared using NP40 lysis buffer (20 mM Tris pH 7.5, 1 mM EDTA, 137 mM NaCl, 10% glycerol and 1% NP40). The amount of protein was quantitated and 10 μg of total lysates were subjected to western analysis.

EC transient transfection and luciferase assay

HUVEC were electroporated using an Amaxa Nucleofector (Amaxa, Gaithersburg, Maryland). Briefly, for optimal transfection 1×10^5 cells were suspended in 100 μl solution V in the presence of 1 μg of pGL2-TK-HRE and subjected to electroporation. After 24 h, medium was changed before treatment under hypoxic condition in hypoxic work station. Luciferase reporter assays were performed in 96-well optiplates (Packard Instrument, Inc., Meriden, CT) using Bright Glo luciferase assay reagents (Promega, Inc., Madison, WI).

siRNA transfection

293 cells were transfected with 50 nM control siRNA or PSMA7 Smart pool siRNA (Dharmacon, Chicago) according to the manufacturer's protocol using DharmaFECT 1 transfection reagent. After 48 h of transfection, total cell lysates were prepared using NP40 lysis buffer.

The PSMA7 smart pool siRNA is a combination of 4 siRNA's and the sequence of each duplex is given below:

Duplex 1, sense: GAAGUAUGUUGCUGAAAUUUU
Antisense: 5′-P.AAUUUCAGCAACAUACUUCUU
Duplex 2, sense: GAAGAGACAUUGUUGUUCUUU
Antisense: 5′-P.AGAACAACAAUGUCUCUUCUU
Duplex 3, sense: GAAGAUCUGUGCUUUGGAUUU
Antisense: 5′-P.AUCCAAAGCACAGAUCUUCUU
Duplex 4, sense: CAUCGUGGGUUUCGACUUUUU
Antisense: 5′-P.AAAGUCGAAACCCACGAUGUU.

Hypoxic treatment

Experiments under hypoxic conditions (1% O_2) were performed in the hypoxic workstation Invivo$_2$ 400 (Biotrace International, Cincinnati, OH). In treatment experiments, cells were treated with EMAP-II (0.5 μg and 1.0 μg), proteasome inhibitor MG132 (20 μM) and prolyl hydroxylase inhibitor DMOG (1 mM) (BioMol, Pennsylvania).

Matrigel angiogenesis assay

All the experiments were performed using growth factor-reduced Matrigel at a concentration of 1 mg/ml (BD Biosciences, Franklin Lakes, NJ), as described [18]. HUVECs (2×10^4 cells per well) were added to the Matrigel-coated plates in a final volume of 200 μl. EMAP-II was added as indicated, and cells were then incubated under hypoxic or normoxic conditions. 16 h later, pictures of each well were taken using a Leica DM IRB inverted microscope equipped with a 40×/0.55 N-PLAN objective lens (Leica, Rockville, MD); pictures were taken with an Olympus DP70 camera (Olympus, Melville, NY) and processed with Bioquant Image Analysis System BQ NOVA PRIME, version 6.75.10 (R&M Biometrics, Nashville, TN). The effect of each treatment was also assessed by measuring the length of cords and the number of junctions formed using the Bioquant Image Analysis System (R&M Biometrics).

Results

EMAP-II binds to ECs through integrin α5β1

HUVEC were incubated with biotinylated EMAP-II and binding was detected using Avidin-FITC by flow cytometry under the non-permeabilized condition (Fig. 1). The background staining by Avidin-FITC and biotinylated BSA is shown (Fig. 1). HUVEC were incubated with EMAP-II and binding was observed at various time points. We observed maximum binding of EMAP-II at 5 min. With increasing incubation time, we observed decreasing cell surface binding by EMAP-II (Fig. 1a). However, binding by biotinylated BSA, the control protein, did not change with increasing incubation time (data not shown). Further, the specificity of binding was examined

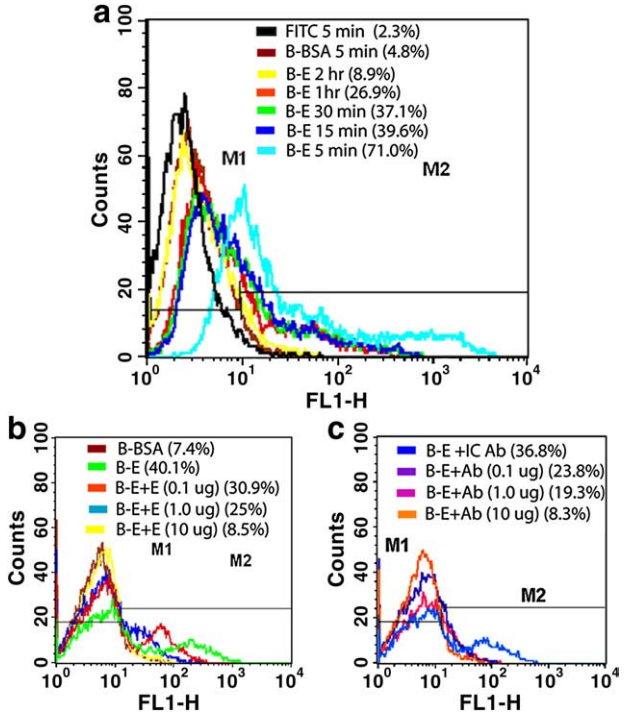

Fig. 1 – EMAP-II binding to endothelial cells. 1×10^5 HUVEC were incubated with 0.5 μg of biotinylated EMAP-II (B-E) for various time points (a) or for 30 min (b and c) and the binding was detected using Avidin-FITC (FITC) by flow cytometry. FITC, biotinylated BSA (B-BSA) and isotype control (IC) antibody were used as controls. In addition to 0.5 μg of B-E, increasing concentrations (0.1 μg, 1.0 μg and 10 μg) of either non-biotinylated EMAP-II (E) (b) or anti-α5β1 (Ab) (c) was added, followed by flow cytometry. The percent binding is shown in the parentheses.

using the combination of biotinylated and increasing amounts of non-biotinylated EMAP-II (Fig. 1b). Non-biotinylated EMAP-II inhibited binding by biotinylated EMAP-II in a concentration dependent manner (Fig. 1b). It has been shown that EMAP-II binds to integrin α5β1 on EC surface [19]. We also observed binding between the two recombinant proteins, EMAP-II and integrin α5β1 (data not shown). In order to confirm that EMAP-II was binding to cell surface integrin α5β1, the binding experiment was carried out in the presence of anti-α5β1 antibody. Compared to isotype control antibody, anti-α5β1 antibody inhibited EMAP-II binding to EC surface in a concentration dependent manner (Fig. 1c). The results indicate that EMAP-II binds to EC surface via integrin α5β1.

Cytoplasmic localization of EMAP-II

In order to determine the cellular fate of cell surface bound EMAP-II, HUVEC were incubated with biotinylated EMAP-II and its presence was detected with Avidin-FITC using an immunofluorescence analysis (Fig. 2). HUVEC treated with biotinylated EMAP-II showed the presence of EMAP-II in the cytoplasm (Fig. 2b). Using biotinylated EMAP-II, we were able to exclude the possibility that the accumulation of EMAP-II in the cytoplasm was due to endogenous EMAP-II. Furthermore, the internalization of biotinylated EMAP-II was specific, as internalization was inhibited by the presence of excess non-biotinylated EMAP-II (Figs. 2c, d). Biotinylated BSA was used as a control (Fig. 2a).

To confirm cytoplasmic localization of EMAP-II in ECs, we incubated EC with EMAP-II and analyzed different endothelial cellular fractions (Fig. 3a). On immunoblotting with an EMAP-II specific antibody, we observed that EMAP-II started accumulating in the cytoplasmic compartment as early as 15 min following incubation (Fig. 3a). There was an increase in the cytoplasmic accumulation of EMAP-II over time, with the maximum accumulation observed at 1 h, and subsequent decrease at the 2 h time point (Fig. 3a). This observation, combined with the timing of cell surface binding of EMAP-II, indicates that EMAP-II binds to the EC surface and is followed by its cytoplasmic internalization.

A small fraction of EMAP-II was detected in the nuclear fractions. We confirmed a complete cellular fractionation procedure and an equal loading by reprobing the same blot with GAPDH (cytoplasmic marker), Cadherin (membrane marker) and histone B (nuclear marker) antibodies (Fig. 3a). Further, we examined the effect of EMAP-II binding to integrin α5β1 on the EC surface to discern EMAP-II's ability to internalize into cytoplasmic compartment of EC. The preincubation of ECs with either an isotype control antibody or non-neutralizing integrin β1 antibody did not affect cytoplasmic accumulation of EMAP-II (Fig. 3b). However, preincubation of ECs with anti-α5β1 antibody inhibited EMAP-II internalization into the cytoplasmic compartment in a dose dependent manner (Fig. 3b). The observed inhibition of EMAP-II internalization may be because of decreased cell surface binding of EMAP-II in the presence of anti-α5β1 antibody.

EMAP-II binds to PSMA7, a component of the proteasome degradation pathway

Next, we focused our studies on the cytoplasmic localization of EMAP-II. In order to identify proteins that may interact with EMAP-

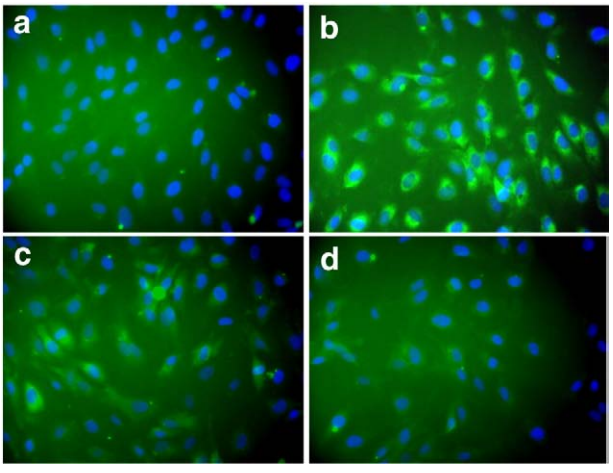

Fig. 2 – EMAP-II internalization in endothelial cells. 1×10^6 HUVEC cells were incubated with 5 μg of biotinylated EMAP-II (B-E) alone (b) or in combination of B-E (5 μg) and non-biotinylated EMAP-II (E); 10 μg (c) and 75 μg (d). The cells were stained with FITC and visualized under immunofluorescent microscope (400×). Biotinylated BSA was used as a control (a). The nuclei were stained blue with DAPI.

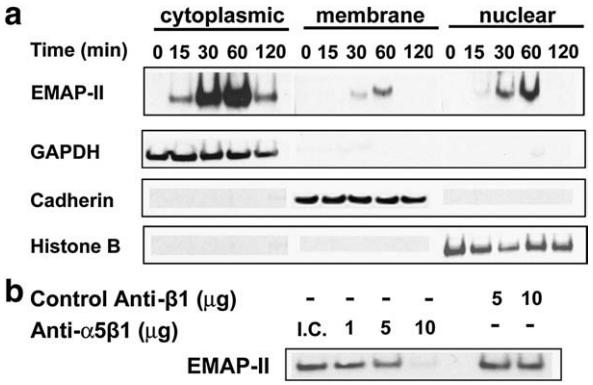

Fig. 3 – Cellular localization of EMAP-II. (a) HUVEC were incubated with EMAP-II for different time points. Cells were fractionated to obtain cytoplasmic, membrane and nuclear fractions and immunoblotted with EMAP-II specific antibody. GAPDH, Cadherin and histone B blotting indicate cytoplasmic, membrane and nuclear fractionation controls and equal loading. (b) HUVEC were incubated either with an isotype control antibody (10 μg) or anti-α5β1 antibody or with anti-β1 antibody for 30 min before incubating with EMAP-II for 15 min. Cells were fractionated to obtain cytoplasmic fraction and immunoblotted with EMAP-II specific antibody.

II in the cytoplasm of ECs, we performed a yeast two-hybrid screen (Supplementary Fig. 1). On the yeast two-hybrid screen, we identified a component of human proteasome subunit, alpha type, 7 (PSMA7) (accession number NM_002792) as a binding partner to EMAP-II.

We confirmed the direct interaction between EMAP-II and PSMA7 using a pull down analysis (Fig. 4a). In the absence of EMAP-II, minimum amounts of PSMA7 was pulled down from the EC lysate; however, addition of increasing amounts of EMAP-II to the reaction pulled down increasing amounts of PSMA7 from the total EC lysate in a concentration dependent manner (Fig. 4a). EMAP-II could pull down PSMA7 from EC lysate indicating binding between the two proteins and confirming the yeast two-hybrid data.

In order to examine which region of PSMA7 is involved in binding with EMAP-II, we used a PSMA7 peptide spot array (Supplementary Fig. 2). Using this approach, we identified two putative regions of PSMA7 (spotted as, spots 41, 42 and 45) that bound to EMAP-II (Supplementary Fig. 2a). Deduced from the spot location, the binding sites were, PLACSPLAAGQSR and RLRHGGSCHV. The background binding is shown (Supplementary Fig. 2b). To provide further confirmation of this binding at a molecular level, we examined the ability of EMAP-II to pull down PSMA7 from EC lysate in the presence of a cocktail of purified binding peptides (Fig. 4b). We synthesized three peptides (test peptides) which bound to EMAP-II on the spot array (spots 41, 42 and 45) and two peptides (control peptides) which did not bind to EMAP-II on the spot array analysis (spots 3 and 50). In the absence of test peptides, EMAP-II could pull down PSMA7 from EC (Fig. 4b, lane 2). However, a cocktail of three test peptides, (41, 42 and 45) inhibited the amount of PSMA7 pulled down by EMAP-II in a concentration dependent manner (Fig. 4b, lanes 3 and 4). At the same tested concentrations, a mixture of control peptides, (3 and 50) did not inhibit PSMA7 pulled down by EMAP-II (Fig. 4b, lanes 5 and 6).

EMAP-II degrades HIF-1α and inhibits the transcriptional activity of HIF-1α through a proteasome-dependent pathway via PSMA7

It has previously been shown that PSMA7 mediates HIF-1α degradation and inhibits its transactivation activity [20]. In the current study, we have demonstrated that EMAP-II binds to PSMA7. In order to determine the biological significance of PSMA7 interaction with EMAP-II, we studied the role of EMAP-II in PSMA7 mediated HIF-1α degradation. In 293 cells, we exogenously overexpressed HIF-α and EMAP-II (Fig. 5). 293 cells express endogenous PSMA7 (data not shown). We achieved about 80% transfection efficiency in these experiments as demonstrated by the control plasmid, pAAV-GFP (data not shown). The experiments were repeated three times. We observed good levels of HIF-1α expression (Fig. 5a, lane 1). However, on co-transfection with EMAP-II, we observed low levels of HIF-1α when compared to the control (Fig. 5a, lanes 2–4 compared to lanes 5–7). The effect of EMAP-II on HIF-1α levels was concentration dependent.

Further, we studied the effect of EMAP-II on the transcriptional activity of HIF-1α in a dual luciferase reporter assay system (Fig. 5b). The transfection of HIF-1α increased the expression of the reporter gene by 7-fold over the basal level. However, on co-transfection, EMAP-II significantly inhibited HIF-1α mediated transcriptional activity when compared to the control (Fig. 5b). Thus, EMAP-II modulated HIF-1α function at the transcriptional level.

It has been shown that HIF-1α degradation occurs via the proteasome degradation pathway through its binding to PSMA7 [20]. To examine whether EMAP-II plays any role in proteasome mediated HIF-1α degradation, we used a broad range proteasome inhibitor, MG132, and accessed HIF-1α levels in 293 cells (Supplementary Fig. 3). In the presence of MG132, EMAP-II did not affect HIF-1α levels (Supplementary Fig. 3). The data indicates that EMAP-II plays a role in proteasome mediated HIF-1α degradation.

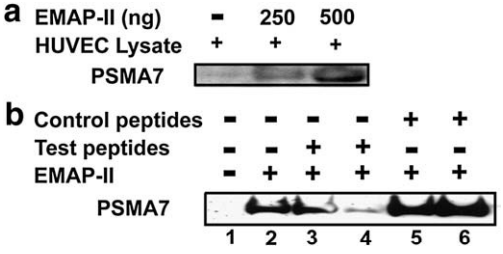

Fig. 4 – EMAP-II binds to PSMA7 protein. (a) The total cell lysate from HUVEC were incubated with different amounts of histidine tagged EMAP-II protein. Following this, nickel agarose beads were added and the EMAP-II bound proteins were pulled down. The bound complexes were immunoblotted using PSMA7 specific antibody. (b) EMAP-II (500 ng) was preincubated either with a cocktail of test peptides (lanes 3 and 4, 1 μM and 10 μM, respectively) or a cocktail of control peptides (lanes 5 and 6, 1 μM and 10 μM, respectively). After incubation with peptides, HUVEC lysate was added followed by the addition of nickel agarose beads. The EMAP-II bound proteins were separated and immunoblotted using PSMA7 specific antibody.

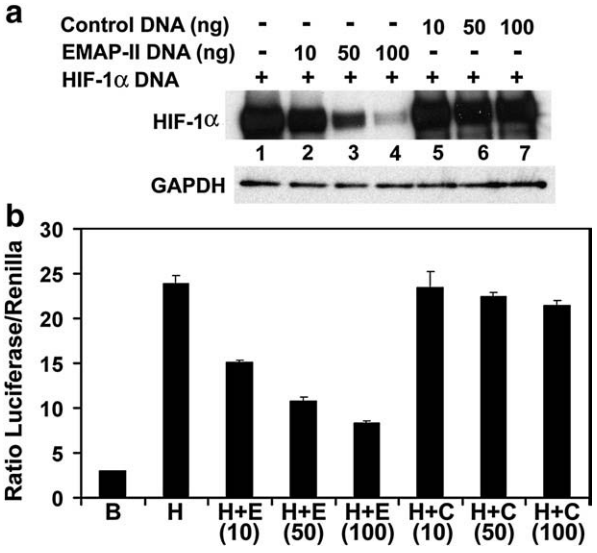

Fig. 5 – EMAP-II regulates HIF-1α protein levels and inhibits HIF-1α mediated transcriptional activity. 293 cells transfected with pFLAG$_3$HIF-1α (50 ng) and various combinations of pAAVEMAP-II DNA or control DNA (10 ng, 50 ng and 100 ng) for 24 h. In dual luciferase reporter assay, cells were additionally transfected with 20 ng of pGL2-TK-HRE and 5 ng of *Renilla* plasmid. (a) Whole cell lysates were prepared and immunoblotted with specific antibody to HIF-1α. GAPDH protein levels show equal loading. (b) After 24 h of transfection, luciferase reporter assays were performed using dual luciferase assay system. Scale bars = standard deviation. The luciferase activity is represented as a ratio of expression levels of luciferase/renilla.

Further, to analyze the role of the proteasomal subunit, PSMA7 in EMAP-II mediated HIF-1α degradation, we downregulated PSMA7 in 293 cells using siRNA and then overexpressed HIF-1α and EMAP-II/control DNA (Fig. 6). The PSMA7 siRNA used was specific and effective in downregulating PSMA7 (Supplementary Fig. 4). As observed before, EMAP-II inhibited HIF-1α protein levels in control siRNA transfected cells (Fig. 6a, lanes 2 and 3 compared to lanes 4 and 5). In contrast, in cells with downregulated PSMA7, EMAP-II failed to degrade HIF-1α (Fig. 6a, lanes 7 and 8). This experiment was repeated three times.

We observed a similar effect of PSMA7 downregulation and EMAP-II on HIF-1α mediated transcriptional activity (Fig. 6b). In the presence of PSMA7 (control siRNA), EMAP-II inhibited HIF-1α mediated transcriptional activity of the reporter gene whereas downregulation of PSMA7 abrogated the ability of EMAP-II to inhibit reporter gene expression (Fig. 6b).

Thus, the data indicate that PSMA7 is required for both EMAP-II mediated HIF-1α degradation and inhibition of its transcriptional activity.

EMAP-II degrades HIF-1α and inhibits its transcriptional activity via the proteasome degradation pathway in ECs

Further, we examined whether EMAP-II mediated HIF-1α degradation and inhibition of its transcriptional activity occurs under physiological conditions in ECs. ECs were grown under normoxic/hypoxic conditions and were treated with EMAP-II (Fig. 7). As expected, we did not observe induction of HIF-1α under normoxic conditions (Fig. 7a, lane 1). In contrast, under hypoxic conditions, there was an increase in HIF-1α protein levels (Fig. 7a, lane 2). However, HIF-1α protein levels were decreased following EMAP-II treatment under hypoxic conditions at both tested concentrations (Fig. 7a, lanes 3 and 4). Thus, EMAP-II could decrease HIF-1α protein levels in ECs under physiologic conditions in a manner similar to what was observed in 293 cells. Further, we studied the role of the proteasome in HIF-1α degradation after EMAP-II treatment of ECs. ECs are difficult to transfect and also show greater variability in transfection efficiency. Hence, instead of using siRNA to downregulate PSMA7, we used a broad range proteasome inhibitor, MG132, in order to obtain more consistent results in these studies. In the presence of MG132, EMAP-II failed to inhibit HIF-1α protein levels indicating that EMAP-II degrades HIF-1α via a proteasome-dependent degradation pathway in ECs (Fig. 7a, lanes 5 and 6). However, under hypoxic conditions, inhibition of the proteasome further stabilized HIF-1α levels (Fig. 7a, lanes 5–7 compared to lane 2). This can be attributed to the broad range of proteasome inhibition by MG132. The results also indicate that there are EMAP-II independent mechanisms involved in the degradation of HIF-1α under hypoxic conditions. Furthermore, we examined whether EMAP-II mediates HIF-1α degradation via a well studied VHL degradation pathway. We inhibited the VHL

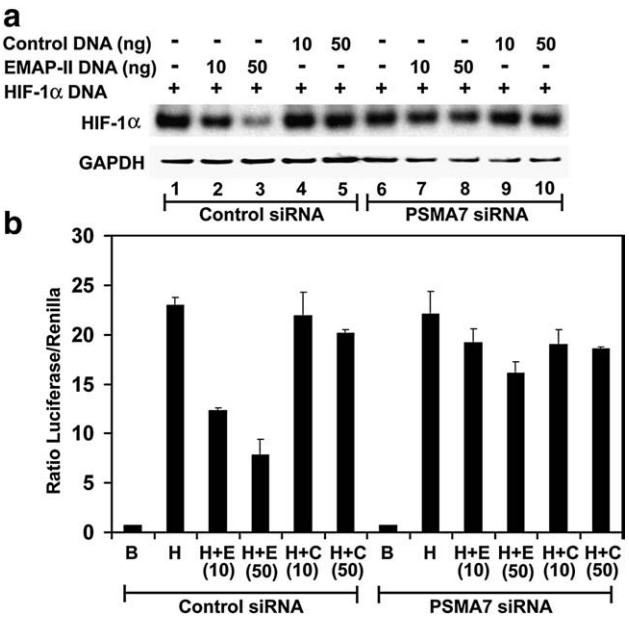

Fig. 6 – EMAP-II mediates HIF-1α degradation and inhibition of its transcriptional activity via PSMA7. 293 cells were transfected with 50 nM PSMA7 specific siRNA or control siRNA for 48 h. After that, cells were transfected with pFLAG$_3$HIF-1α (50 ng) and various combinations of pAAVEMAP-II DNA or control DNA (10 ng, 50 ng and 100 ng) for 24 h. In dual luciferase reporter assay, cells were additionally transfected with 20 ng of pGL2-TK-HRE and 5 ng of *Renilla* plasmid. (a) Whole cell lysates were prepared and immunoblotted with specific antibody to HIF-1α. GAPDH protein levels show equal loading. (b) After 24 h of transfection, luciferase reporter assays were performed using dual luciferase assay system. Scale bars = standard deviation. The luciferase activity is represented as a ratio of expression levels of luciferase/renilla.

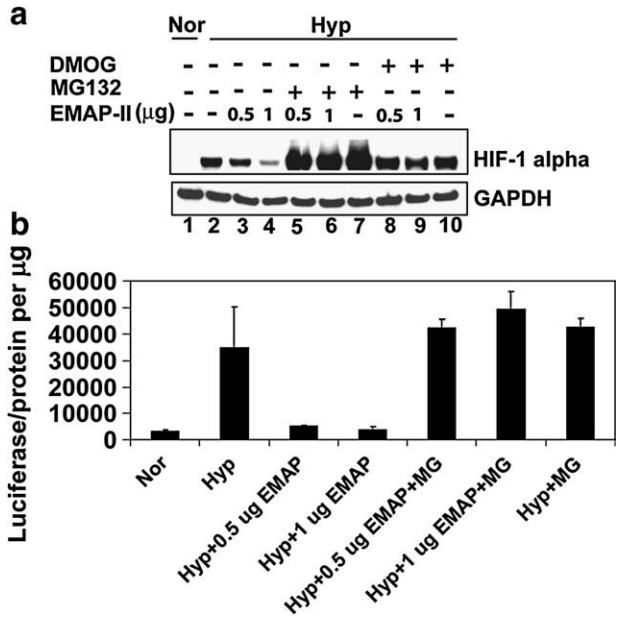

Fig. 7 – EMAP-II mediates HIF-1α degradation and inhibition of HIF-1α transcriptional activity via the proteasome degradation pathway in endothelial cells. (a) HUVEC were grown either under normoxia (20% oxygen) (lanes 1) or hypoxia (1% oxygen) (lanes 2–10) and treated with EMAP-II, MG132 (20 μM) and DMOG (1 mM) as indicated. The lysates were prepared and immunoblotted against HIF-1α antibody. The GAPDH control shows equal loading. (b) HUVEC were electroporated with 1 μg of pGL2-TK-HRE DNA using an Amaxa Nucleofector. After 24 h, cells were treated with 20 μM MG132 (MG) and EMAP-II as indicated and grown either under normoxic (Nor) (20% oxygen) or hypoxic (Hyp) (1% oxygen) conditions. Luciferase reporter assays were performed in 96-well optiplates using Bright Glo luciferase assay reagents. Scale bars = standard deviation.

mediated HIF-1α degradation pathway using the prolyl hydroxylase inhibitor, DMOG. In the presence of DMOG, EMAP-II could not degrade HIF-1α (Fig. 7a, lanes 8 and 9). The data suggest that EMAP-II might be one of the players in the multicomponent VHL proteasomal degradation pathway involving HIF-1α degradation. However, DMOG could stabilize HIF-1α in the absence of EMAP-II indicating that there are EMAP-II independent VHL proteasomal degradation pathways (Fig. 7a, lane 10).

Next, we examined the role of EMAP-II in the transactivation function of HIF-1α in ECs using a luciferase reporter assay system (Fig. 7b). Compared to normoxia, we observed a significant increase in luciferase activity under hypoxic conditions indicating HIF-1α mediated transactivation of the reporter gene. The HIF-1α mediated transactivation was inhibited following treatment with EMAP-II (Fig. 7b). However, the EMAP-II mediated inhibition of transcription was abolished by treatment with MG132 (Fig. 7b). The results suggest that in ECs, EMAP-II inhibits HIF-1α transactivation by regulating HIF-1α levels via a proteasomal degradation pathway.

EMAP-II inhibits EC cord formation under hypoxic conditions

To examine the physiological significance of the regulation of HIF-1α activity by EMAP-II, we analyzed angiogenic cord formation in ECs, one of the important functions of HIF-1α. ECs cultured under hypoxic conditions in growth factor depleted medium form tube like structures in contrast to cells growing under normoxic conditions (Figs. 8, a and b). The EC cord formation was completely inhibited by EMAP-II treatment under hypoxic conditions (Figs. 8, c and d). However, the effect of EMAP-II on cord formation was abolished by treatment with MG132 (Figs. 8, e and f). The length of the cords and the number of cord junctions were measured and quantitated (Figs. 8, g and h). Cells grown under hypoxia showed longer cords compared to cells treated with EMAP-II (Fig. 8g). The effect of EMAP-II on cord length was abolished in the presence of MG132 under hypoxic conditions. A similar pattern was observed with the number of cord junctions in each treatment group (Fig. 8h). The data indicate that EMAP-II inhibits angiogenic cord formation via regulation of HIF-1α activity in ECs.

Discussion

The regulation of angiogenesis by hypoxia is an important component of normal vascular homeostasis [21,22]. Under pathological conditions such as cancer, hypoxia results in the upregulation of the angiogenesis-stimulating factor HIF-1α. HIF-1α induces angiogenesis which is critical for tumor cell proliferation and survival [22]. Under similar conditions, various cell types (monocytes, macrophages and tumor cells) secret EMAP-II, a multifunctional cytokine cleaved from its precursor Pro-EMAP. EMAP-II has been shown to have anti-angiogenic properties including the inhibition of EC proliferation, tube formation, adhesion to fibronectin and induction of EC apoptosis [8,19] (Fig. 9). In the present series of studies, we explored how EMAP-II exerts some of its anti-angiogenic activities on ECs. Our results indicate that EMAP-II regulates HIF-1α activity, resulting in the inhibition of angiogenic cord formation in ECs. This is depicted schematically in Fig. 9.

To gain an insight into the mechanism of anti-angiogenic activity of EMAP-II, we carried out a series of investigations to elucidate the fate of cell surface bound EMAP-II. We studied the downstream biochemical and molecular effects of EMAP-II on ECs. It has been shown that EMAP-II binds to different EC surface molecules to exert some of its activities. EMAP-II inhibits EC proliferation by binding to ATP synthase whereas it inhibits EC adhesion and spreading via direct binding to integrin α5β1 (Fig. 9) [16,19]. In the present study, we confirmed EMAP-II binding to integrin α5β1 on ECs. Cell surface integrin receptors play an important role in regulating vascular growth [23]. The anti-angiogenic proteins endostatin and tumstatin exert their effects through α5β1 and αvβ3 receptors, respectively [24,25]. Our data showed that after binding to the cell surface of ECs, the majority of EMAP-II was internalized into the cytoplasmic compartment. Although, we also observed low levels of EMAP-II in the nucleus, in the present study we focused on the role of cytoplasmic EMAP-II. Preincubation of ECs with anti-α5β1 antibody inhibited EMAP-II cell surface binding and subsequent internalization into the cytoplasm indicating that α5β1 is the cell surface binding receptor for EMAP-II on ECs. However, it is possible that integrin α5β1 may also play a role in the internalization process of EMAP-II. It has been demonstrated that β1 integrins, including α5β1, play an important role in endocytosis and turnover of the extracellular matrix component fibronectin via caveolin-1 [26,27].

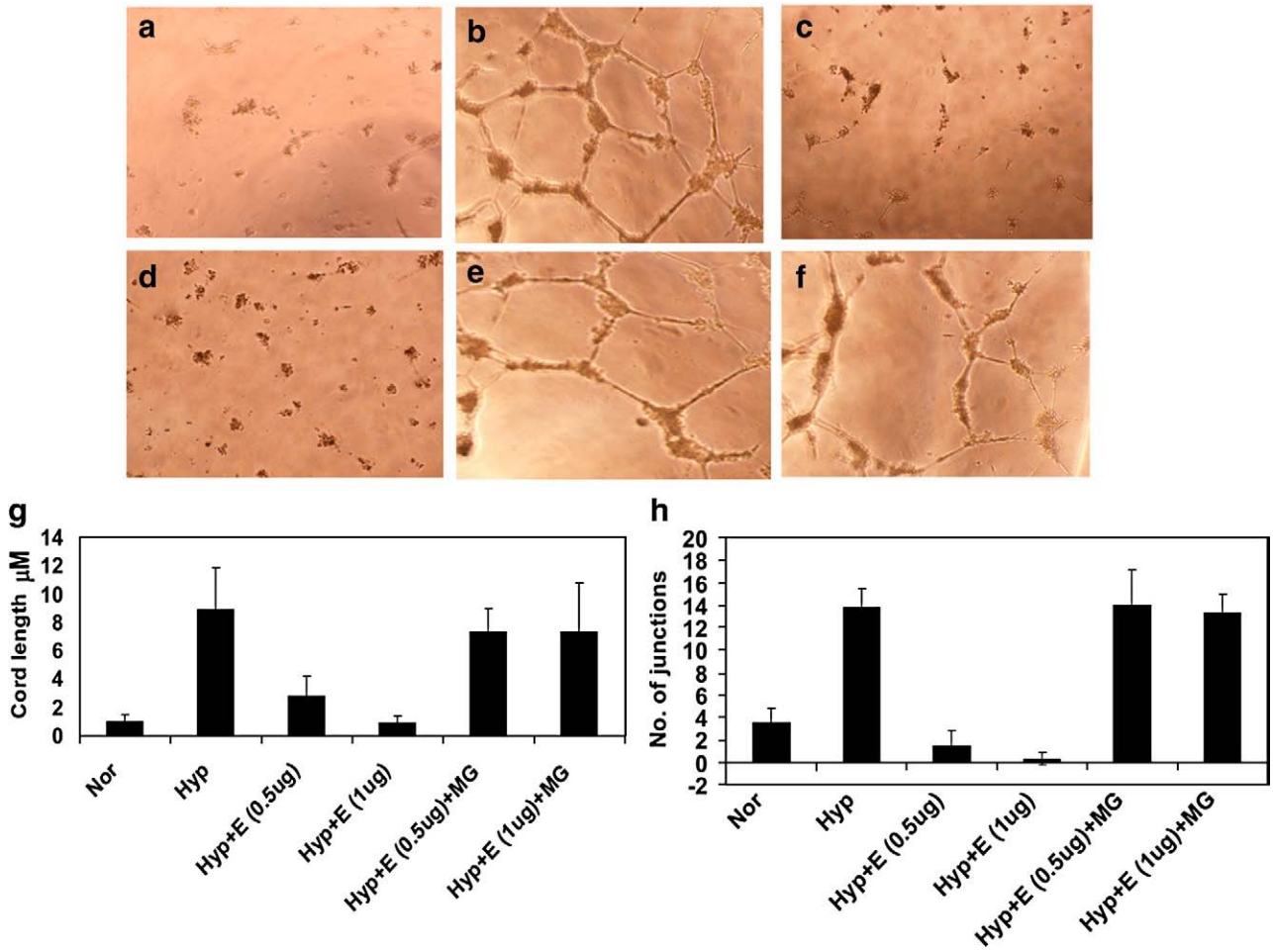

Fig. 8 – EMAP-II inhibits HIF-1α induced cord formation. HUVEC were plated onto the growth factor-reduced Matrigel-coated plates (2×10^4 cells per well) and 0.5 μg (c and e) and 1.0 μg (d and f) EMAP-II was added followed by 20 μM MG132 (MG) (e and f). Cells were then incubated under normoxic (Nor) (20% oxygen) (a) or hypoxic (Hyp) (1% oxygen) (b–f) conditions. 16 h later, each well was photographed using a Leica DM IRB inverted microscope equipped with a 40×/0.55 N-PLAN objective lens and Olympus DP70 camera (a–f). The effect of each treatment was assessed by measuring the length of cords (g) and the number of junctions (h) formed using the Bioquant Image Analysis system. Scale bars = standard deviation.

Further, to elucidate whether EMAP-II interacts with any cytoplasmic proteins to exert its effect, we utilized a yeast two-hybrid system. We identified PSMA7, one of the components of the proteasome degradation pathway as a binding partner for EMAP-II. The 26S proteasome complex is a ubiquitous multi-catalytic protease complex composed of the 20S catalytic core complex and the 19S regulatory complex [28]. The polyubiquitinated protein substrates are degraded inside the 20S core complex. PSMA7, an α-type subunit of the 20S proteasome core complex, physically interacts with HIF-1α and inhibits the transactivation activity of HIF-1α by causing the proteasome-dependent degradation of HIF-1α [20]. Given the published role of PSMA7 in HIF-1α degradation and our observation that PSMA7 binds to EMAP-II, we next examined whether EMAP-II is involved in HIF-1α regulation through the proteasome. Using a proteasome inhibitor, we demonstrated that EMAP-II mediates HIF-1α degradation via the proteasome and PSMA7 is required for this process. This was because downregulation of PSMA7 abolished EMAP-II mediated HIF-1α degradation as well as its transactivation function. Although PSMA7 is required for EMAP-II mediated HIF-1α regulation, we do not know whether the physical binding between EMAP-II and PSMA7 is necessary for this process to occur. The remarkable plasticity of HIF-1α, its importance in the vascular system, and the number of different proteins that regulate this process indicate that there also exist EMAP-II independent HIF-1α degradation pathways [15]. The von Hippel–Lindau (VHL) ubiquitination degradation pathway of HIF-1α degradation has been well elucidated [29–31]. A number of different proteins regulate this process [15]. Our findings indicate that EMAP-II may be a part of the multicomponent VHL-proteasome ubiquitination pathway while there are also EMAP-II independent VHL proteasomal degradation pathways that exist. Thus, there is a large repertoire of different molecular pathways involved in HIF-1α regulation. This is not surprising, given the vast diversity of genes regulated by HIF-1α [4]. We are currently examining the exact role of EMAP-II in the VHL-proteasome ubiquitination pathway of HIF-1α degradation.

In the current study, we have demonstrated the direct consequence of HIF-1α degradation by EMAP-II. It has been shown that under hypoxic conditions, ECs cultured in the absence of growth factors survive and form tube like structures via HIF-1α expression [8,18,32]. We also know that EMAP-II inhibits angiogenesis via inhibition of

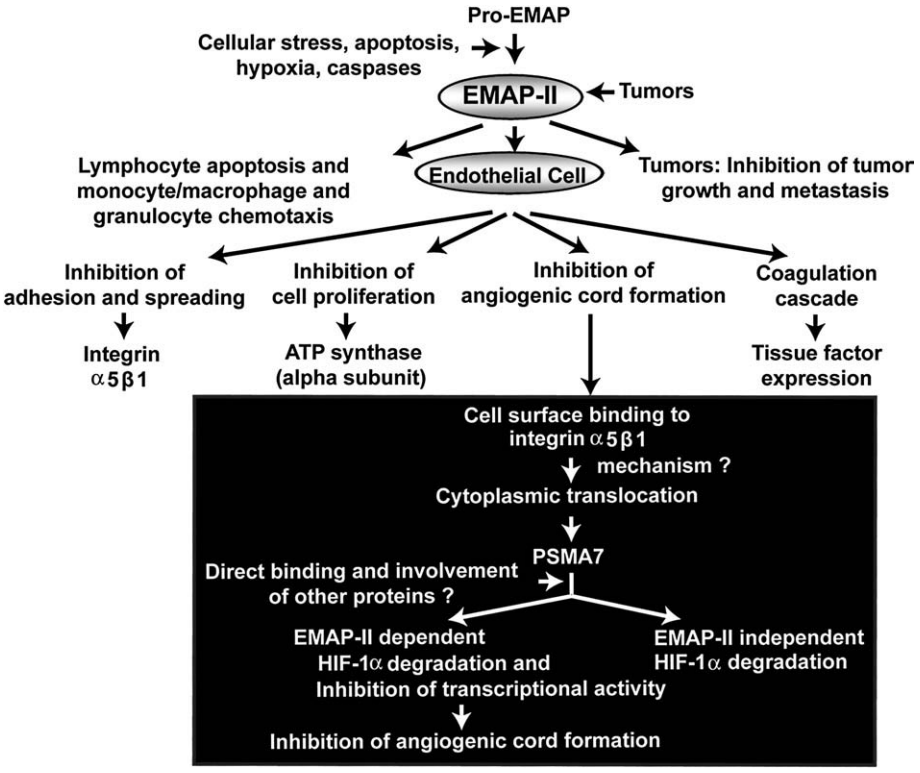

Fig. 9 – EMAP-II, a multifunctional cytokine has potent effects on endothelial cells. The molecular mechanism and the functional consequence of EMAP-II mediated HIF-1α regulation presented in this study is depicted (black box).

angiogenic cord formation by ECs [8,18,32]. Here we show that EMAP-II inhibits angiogenic cord formation by regulation of HIF-1α. The newly formed angiogenic cords are the basis of angiogenesis in growing tumors. Tumor progression is dependent on its ability to establish a vascular network [33]. HIF-1α, an important player in tumor angiogenesis, has been reported in a variety of human cancers [34]. A number of genes involved in the control of growth signaling, cell survival and invasion were found to be induced directly or indirectly by HIF-1α [6]. HIF-1α plays a critical role in tumor angiogenesis by activating angiogenic growth factors including VEGF and mediates a cell-autonomous transcriptional response in human ECs [35–37]. Hypoxic cells are more resistant to ionizing radiation and chemotherapy, are more invasive and metastatic, resistant to apoptosis, and genetically unstable [38]. Thus, HIF-1α is emerging as a common target underlying the different aspects of tumor progression. Our finding that EMAP-II regulates HIF-1α activities may result in wide-ranging applications for EMAP-II in several therapeutic regimens.

Acknowledgments

This research was supported [in part] by the Intramural Research Program of the NIH, National Cancer Institute, Center for Cancer Research.

Appendix A. Supplementary data

Supplementary data associated with this article can be found, in the online version, at doi:10.1016/j.yexcr.2009.03.021.

REFERENCES

[1] P. Carmeliet, Angiogenesis in life, disease and medicine, Nature 438 (2005) 932–936.
[2] R.K. Jain, Molecular regulation of vessel maturation, Nat. Med. 9 (2003) 685–693.
[3] G.L. Semenza, Regulation of mammalian O2 homeostasis by hypoxia-inducible factor 1, Annu. Rev. Cell Dev. Biol. 15 (1999) 551–578.
[4] G.L. Semenza, Targeting HIF-1 for cancer therapy, Nat. Rev., Cancer 3 (2003) 721–732.
[5] D. Shweiki, A. Itin, D. Soffer, E. Keshet, Vascular endothelial growth factor induced by hypoxia may mediate hypoxia-initiated angiogenesis, Nature 359 (1992) 843–845.
[6] L. Marignol, M. Coffey, M. Lawler, D. Hollywood, Hypoxia in prostate cancer: a powerful shield against tumour destruction? Cancer Treat. Rev. 34 (2008) 313–327.
[7] J. Kao, J. Ryan, G. Brett, J. Chen, H. Shen, Y.G. Fan, G. Godman, P.C. Familletti, F. Wang, Y.C. Pan, D. Stern, M. Clauss, Endothelial monocyte-activating polypeptide II. A novel tumor-derived polypeptide that activates host-response mechanisms, J. Biol. Chem. 267 (1992) 20239–20247.
[8] A.C. Berger, H.R. Alexander, G. Tang, P.S. Wu, S.M. Hewitt, E. Turner, E. Kruger, W.D. Figg, A. Grove, E. Kohn, D. Stern, S.K. Libutti, Endothelial monocyte activating polypeptide II induces endothelial cell apoptosis and may inhibit tumor angiogenesis, Microvasc. Res. 60 (2000) 70–80.
[9] A.C. Berger, H.R. Alexander, P.C. Wu, G. Tang, M.F. Gnant, A. Mixon, E.S. Turner, S.K. Libutti, Tumour necrosis factor receptor I (p55) is upregulated on endothelial cells by exposure to the tumour-derived cytokine endothelial monocyte-activating polypeptide II (EMAP-II), Cytokine 12 (2000) 992–1000.
[10] R. van Horssen, A.M. Eggermont, T.L. ten Hagen, Endothelial monocyte-activating polypeptide-II and its functions in (patho)

physiological processes, Cytokine Growth Factor Rev. 17 (2006) 339–348.
[11] M.F. Gnant, A.C. Berger, J. Huang, M. Puhlmann, P.C. Wu, M.J. Merino, D.L. Bartlett, H.R. Alexander Jr., S.K. Libutti, Sensitization of tumor necrosis factor alpha-resistant human melanoma by tumor-specific in vivo transfer of the gene encoding endothelial monocyte-activating polypeptide II using recombinant vaccinia virus, Cancer Res. 59 (1999) 4668–4674.
[12] L. Crippa, A. Gasparri, A. Sacchi, E. Ferrero, F. Curnis, A. Corti, Synergistic damage of tumor vessels with ultra low-dose endothelial-monocyte activating polypeptide-II and neovasculature-targeted tumor necrosis factor-alpha, Cancer Res. 68 (2008) 1154–1161.
[13] R. van Horssen, J.A. Rens, F. Brunstein, V. Guns, M. van Gils, T.L. Hagen, A.M. Eggermont, Intratumoural expression of TNF-R1 and EMAP-II in relation to response of patients treated with TNF-based isolated limb perfusion, Int. J. Cancer 119 (2006) 1481–1490.
[14] A.T. Tandle, C. Mazzanti, H.R. Alexander, D.D. Roberts, S.K. Libutti, Endothelial monocyte activating polypeptide-II induced gene expression changes in endothelial cells, Cytokine 30 (2005) 347–358.
[15] J.H. Baek, P.C. Mahon, J. Oh, B. Kelly, B. Krishnamachary, M. Pearson, D.A. Chan, A.J. Giaccia, G.L. Semenza, OS-9 interacts with hypoxia-inducible factor 1alpha and prolyl hydroxylases to promote oxygen-dependent degradation of HIF-1alpha, Mol. Cell 17 (2005) 503–512.
[16] S.Y. Chang, S.G. Park, S. Kim, C.Y. Kang, Interaction of the C-terminal domain of p43 and the alpha subunit of ATP synthase. Its functional implication in endothelial cell proliferation, J. Biol. Chem. 277 (2002) 8388–8394.
[17] A. Rapisarda, B. Uranchimeg, D.A. Scudiero, M. Selby, E.A. Sausville, R.H. Shoemaker, G. Melillo, Identification of small molecule inhibitors of hypoxia-inducible factor 1 transcriptional activation pathway, Cancer Res. 62 (2002) 4316–4324.
[18] M. Calvani, A. Rapisarda, B. Uranchimeg, R.H. Shoemaker, G. Melillo, Hypoxic induction of an HIF-1alpha-dependent bFGF autocrine loop drives angiogenesis in human endothelial cells, Blood 107 (2006) 2705–2712.
[19] M.A. Schwarz, H. Zheng, J. Liu, S. Corbett, R.E. Schwarz, Endothelial-monocyte activating polypeptide II alters fibronectin based endothelial cell adhesion and matrix assembly via alpha5 beta1 integrin, Exp. Cell Res. 311 (2005) 229–239.
[20] S. Cho, Y.J. Choi, J.M. Kim, S.T. Jeong, J.H. Kim, S.H. Kim, S.E. Ryu, Binding and regulation of HIF-1alpha by a subunit of the proteasome complex, PSMA7, FEBS Lett. 498 (2001) 62–66.
[21] A.J. Giaccia, M.C. Simon, R. Johnson, The biology of hypoxia: the role of oxygen sensing in development, normal function, and disease, Genes Dev. 18 (2004) 2183–2194.
[22] K. Hirota, G.L. Semenza, Regulation of angiogenesis by hypoxia-inducible factor 1, Crit. Rev. Oncol./Hematol. 59 (2006) 15–26.
[23] S.E. Francis, K.L. Goh, K. Hodivala-Dilke, B.L. Bader, M. Stark, D. Davidson, R.O. Hynes, Central roles of alpha5beta1 integrin and fibronectin in vascular development in mouse embryos and embryoid bodies, Arterioscler. Thromb. Vasc. Biol. 22 (2002) 927–933.
[24] Y. Maeshima, P.C. Colorado, R. Kalluri, Two RGD-independent alpha vbeta 3 integrin binding sites on tumstatin regulate distinct anti-tumor properties, J. Biol. Chem. 275 (2000) 23745–23750.
[25] A. Sudhakar, H. Sugimoto, C. Yang, J. Lively, M. Zeisberg, R. Kalluri, Human tumstatin and human endostatin exhibit distinct antiangiogenic activities mediated by alpha v beta 3 and alpha 5 beta 1 integrins, Proc. Natl. Acad. Sci. U. S. A. 100 (2003) 4766–4771.
[26] J. Sottile, J. Chandler, Fibronectin matrix turnover occurs through a caveolin-1-dependent process, Mol. Biol. Cell 16 (2005) 757–768.
[27] F. Shi, J. Sottile, Caveolin-1-dependent {beta}1 integrin endocytosis is a critical regulator of fibronectin turnover, J. Cell. Sci. 121 (2008) 2360–2371.
[28] W.L. Gerards, W.W. de Jong, W. Boelens, H. Bloemendal, Structure and assembly of the 20S proteasome, Cell. Mol. Life Sci. 54 (1998) 253–262.
[29] P.H. Maxwell, M.S. Wiesener, G.W. Chang, S.C. Clifford, E.C. Vaux, M.E. Cockman, C.C. Wykoff, C.W. Pugh, E.R. Maher, P.J. Ratcliffe, The tumour suppressor protein VHL targets hypoxia-inducible factors for oxygen-dependent proteolysis, Nature 399 (1999) 271–275.
[30] P.J. Kallio, W.J. Wilson, S. O Brien, Y. Makino, L. Poellinger, Regulation of the hypoxia-inducible transcription factor 1alpha by the ubiquitin-proteasome pathway, J. Biol. Chem. 274 (1999) 6519–6525.
[31] C.H. Sutter, E. Laughner, G.L. Semenza, Hypoxia-inducible factor 1alpha protein expression is controlled by oxygen-regulated ubiquitination that is disrupted by deletions and missense mutations, Proc. Natl. Acad. Sci. U. S. A. 97 (2000) 4748–4753.
[32] M.A. Schwarz, J. Kandel, J. Brett, J. Li, J. Hayward, R.E. Schwarz, O. Chappey, J.L. Wautier, J. Chabot, P. Lo Gerfo, D. Stern, Endothelial-monocyte activating polypeptide II, a novel antitumor cytokine that suppresses primary and metastatic tumor growth and induces apoptosis in growing endothelial cells, J. Exp. Med. 190 (1999) 341–354.
[33] D. Hanahan, J. Folkman, Patterns and emerging mechanisms of the angiogenic switch during tumorigenesis, Cell 86 (1996) 353–364.
[34] H. Zhong, A.M. De Marzo, E. Laughner, M. Lim, D.A. Hilton, D. Zagzag, P. Buechler, W.B. Isaacs, G.L. Semenza, J.W. Simons, Overexpression of hypoxia-inducible factor 1alpha in common human cancers and their metastases, Cancer Res. 59 (1999) 5830–5835.
[35] J.A. Forsythe, B.H. Jiang, N.V. Iyer, F. Agani, S.W. Leung, R.D. Koos, G.L. Semenza, Activation of vascular endothelial growth factor gene transcription by hypoxia-inducible factor 1, Mol. Cell. Biol. 16 (1996) 4604–4613.
[36] D.J. Manalo, A. Rowan, T. Lavoie, L. Natarajan, B.D. Kelly, S.Q. Ye, J.G. Garcia, G.L. Semenza, Transcriptional regulation of vascular endothelial cell responses to hypoxia by HIF-1, Blood 105 (2005) 659–669.
[37] N. Tang, L. Wang, J. Esko, F.J. Giordano, Y. Huang, H.P. Gerber, N. Ferrara, R.S. Johnson, Loss of HIF-1alpha in endothelial cells disrupts a hypoxia-driven VEGF autocrine loop necessary for tumorigenesis, Cancer Cell 6 (2004) 485–495.
[38] G. Melillo, Inhibiting hypoxia-inducible factor 1 for cancer therapy, Mol. Cancer Res. 4 (2006) 601–605.